

COMPARISON ON URBAN CLASSIFICATIONS USING LANDSAT-TM AND LINEAR SPECTRAL MIXTURE ANALYSIS EXTRACTED IMAGES: NAKHON RATCHASIMA MUNICIPAL AREA, THAILAND

Sunya Sarapirome* and Chotipa Kulrat

Received: Jun 6, 2010; Revised: Sept 10, 2010; Accepted: Sept 14, 2010

Abstract

The objective of this research was to compare accuracies of urban land-use classifications of Nakhon Ratchasima municipality and the surrounding area using different types of images and classification methods. Fraction images of green vegetation (V), impervious surface (I), soil (S), and shade (Sh) were generated using Linear Spectral Mixture Analysis (LSMA) with input of their spectral signatures extracted from a scatter-plot of Thematic Mapper (TM) images transformation using Principle Component Analysis (PCA). This resulted in 2 sets of fraction images i.e. V-I-S and V-S-Sh. These 2 sets of fraction images were classified by Maximum Likelihood Classification (MLC) and Endmember Classification (EMC) methods while the original TM images were classified by MLC. Accuracies of 5 resulting urban land-use maps of the study area were assessed by means of error matrix using checking data from field investigation and large-scale color air photos. The assessment revealed that all maps derived from fraction images showed a higher overall accuracy and Kappa statistic than the ones from the original TM images. MLC of the set of V-I-S fraction images provided the highest overall accuracy (72.21%) and MLC of the original TM images provided the lowest overall accuracy (66.93%). Accuracies of land-use classes from the different methods and sets of images based on producer's and user's accuracies were reported and discussed.

Keywords: Urban area classification, LSMA, EMC, fraction images, TM images

Introduction

Urban areas have grown constantly and rapidly due to economic and population expansion. The growth may cause an adverse impact on the environment such as air pollution, sound pollution, traffic jams, and quality of life degradation. Therefore, information on urban change is considered important in

managing and planning for future development.

Remote sensing technology is a potential tool for monitoring the urban change dynamically. In general, the usage of high-spatial resolution remote sensing data such as QuickBird, IKONOS, and large-scale air photos can give better results for urban land-use classification

School of Remote Sensing, Institute of Science, Suranaree University of Technology, 111 University Avenue, Muang District, Nakhon Ratchasima 30000, Thailand. E-mail: sunyas@sut.ac.th

** Corresponding author*

because of the spatial complexity of components in the urban area such as buildings, roads, runways, vegetation, concrete, asphalt, and soil. An urban component covering a small area cannot be detected in the low- to medium-spatial resolution data because it can mix with other components within a pixel. Since high-spatial resolution data have been costly, many researchers have concentrated on improving the accuracy of urban land-use classification using medium-spatial resolution remote sensing data, e.g. Landsat Thematic Mapper (TM) and Enhance Thematic Mapper plus (ETM⁺). However, the problem is that a pixel of these data is too coarse to separate each component in an urban environment (Lu and Weng, 2004). Also, in the traditional classification approaches such as Maximum Likelihood Classification (MLC) and Minimum Distance to Mean Classification (MDMC) it is assumed that an image pixel has only 1 land-use class. Due to the complex combination in an image pixel of an urban or sub-urban area, its spectral reflectance may represent the combination of several land-use types and it is called a mixed pixel (Wu, 2004). A mixed pixel can have a problem effect on land-use classification accuracy.

To improve classification accuracy, advanced methods have been sought to improve the TM data, particularly in a heterogeneous area like an urban area. Linear Spectral Mixture Analysis (LSMA) has been the well-known approach often used to handle the mixed pixel problem (Adams *et al.*, 1995; Ridd, 1995; Plaza *et al.*, 2002; Wu and Murray, 2003; Lu and Weng, 2004; Wu, 2004). The method assumed that, within a pixel, the spectrum measured by the sensor is the linear combination of the spectral reflectance of all components (endmembers) within it and the proportion of an endmember represents the proportion of the area covered by the feature(s) of that component on the ground (Lu and Weng, 2006). LSMA involves 2 steps, i.e. to find the unique spectral signatures of pure ground components (endmembers) and to generate fraction images by inputting the unique spectral signatures of pure ground

components into the LSMA equation. The spectral of pure ground components can be achieved by Principal Component Analysis (PCA) or Minimum Noise Fraction (MNF) transformation, spectral signature library, and laboratory. Each pixel of a fraction image of a component shows a percentage of the area covered by the component contained in a pixel. A number of fraction images depend on a number of pure reflectance signatures of endmembers input to the LSMA equation. There are several endmember combinations used for fraction image generation such as vegetation-impervious surface-soil (V-I-S) combination (Ridd, 1995; Phinn *et al.*, 2002; Wu, 2004), low albedo-high albedo-vegetation (Small, 2001), and vegetation-soil-shade (V-S-Sh) combination (Lu and Weng, 2004).

Apart from TM data improvement for better accuracy of urban classification, researches have been reported on the usage of new or advanced methods for urban land-use classification through fraction images e.g. Thresholds Classification (Lu *et al.*, 2003), Endmember Model Classification (EMC) (Ridd, 1995; Lu and Weng, 2004; Kulrat, 2008), and expert system (Lu and Weng, 2006). These methods commonly employ fraction images as input and rely on data from the Areas of Interest (AOIs). The first one designs thresholds for each class based on statistics (standard deviation, mean, etc.) of fraction images with respect to the class. The second one defines each class based on the combination of certain ranges of 3 endmembers. The last one additionally takes other parameters such as population density and high and low albedo into consideration.

In this research, LSMA was applied to Landsat5 TM images, covering the urban and surrounding areas of Nakhon Ratchasima municipality in the northeast of Thailand, to generate 2 sets of fraction images which were V-I-S and V-S-Sh. These fraction images and the original TM images were further employed for land-use classification of the study area. In addition to MLC which was applied to all those images, EMC was employed for fraction images as well. The classification accuracies

on using TM images, V-I-S, and V-S-Sh fraction images by means of MLC and using V-I-S and V-S-Sh fraction images by EMC were estimated through an error matrix and then compared. The conceptual diagram of the study is shown in Figure 1.

Study Area

Nakhon Ratchasima municipality and the surrounding area (Figure 2), located in the northeast of Thailand, was selected as the study area. It has an area about 95 km² covering a Central Business District (CBD), low and medium density residential areas and a partly agricultural area. Its typical urban land-use pattern could be found in any fast-growing towns in the northeast or elsewhere in Thailand. Nakhon Ratchasima province is the spatially largest and the second biggest

population province of Thailand and is considered as the front door to the Northeast. The study area has encountered a rapid urban environment and population growth. Around 20% of the municipal area is covered by CBD, low and medium density residential areas, and horticulture. The other 80% of the outer areas are low density residential areas, agricultural areas such as paddy fields and horticulture, forest, bare soil, and shrub. Photos of these land-use units from the area are displayed in Figure 3. Accurate land-use classification particularly in the urban area can assist in monitoring urban expansion and controlling or planning its future development.

Concept of LSMA

LSMA is a model assuming that the spectral reflection of a given pixel measured by the

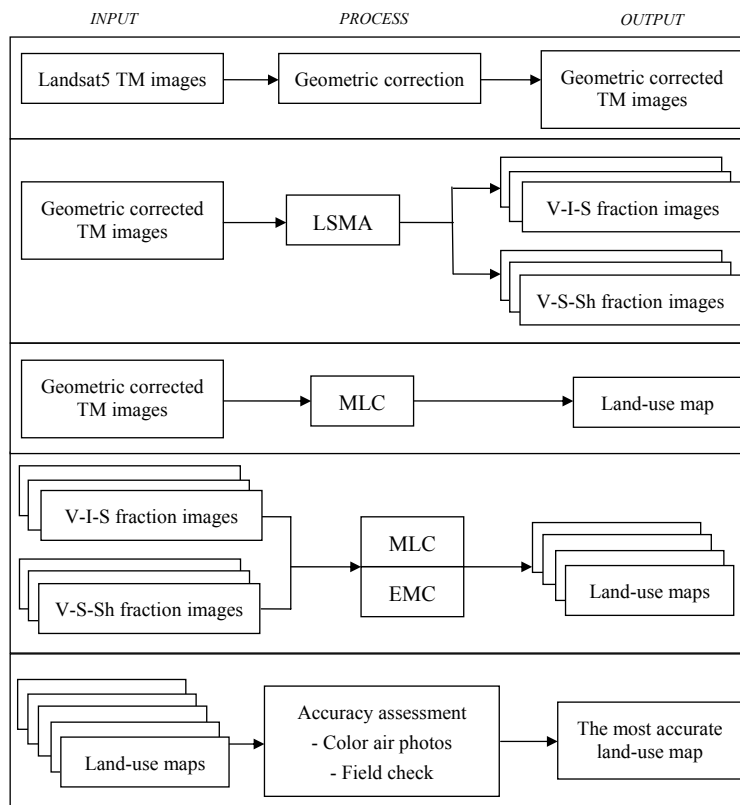


Figure 1. Conceptual diagram of the study

sensor is a linear combination of the spectral reflectance of all components within the pixel. Any component contained in a pixel is called an endmember. The endmembers can be types of land use or types of physical properties of features. These include green vegetation, impervious surfaces (e.g. buildings, roads, runways, concrete), soil, shade, non-photosynthesis (e.g. dry leaves, dry branches, dry grass), high albedo (e.g. concrete, clouds,

sand), and low albedo (e.g. water, asphalt). Fractions of endmembers represent proportions of the areas covered by distinct features on the ground that appeared in a pixel of an image (Lu and Weng, 2006). Thus, within a pixel of an image, features on the ground will more relate to fractions of endmembers than to the total reflectance. Then, direct use of fraction images for land-use classification could obtain a more accurate result.

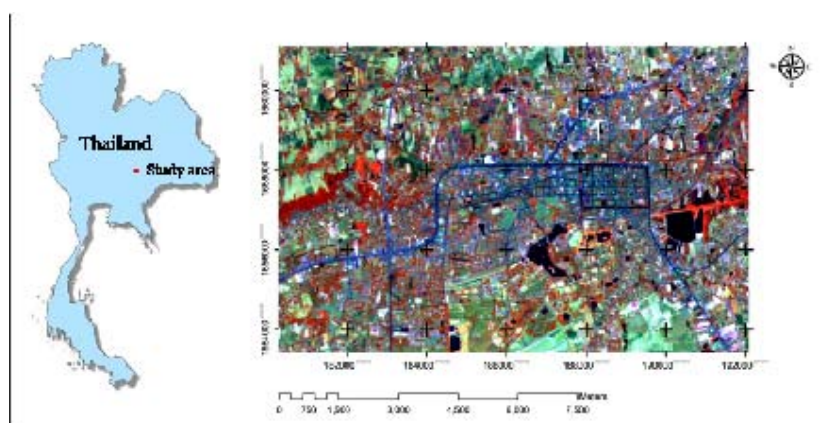


Figure 2. False color composite image (RGB:453) of Landsat5 TM data of the study area

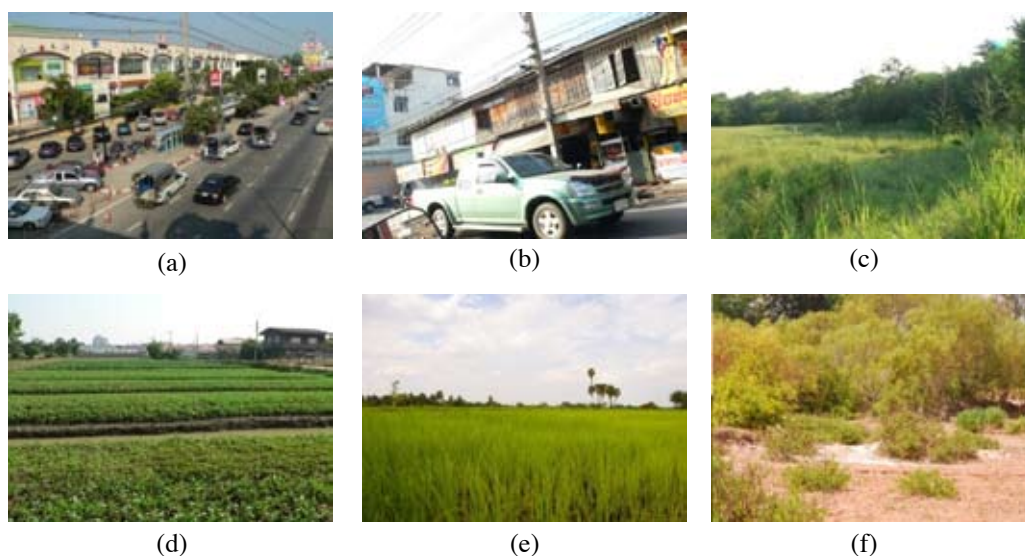


Figure 3. Photos showing (a) CBD, (b) residential area, (c) grass field with forest in the back, (d) horticultural area, (e) paddy field, and (f) shrub with bare land in the front

The LSMA equation is the expression of the linear combination of the endmember reflectance of a mixed pixel as shown in equation (1) (Adams *et al.*, 1995).

$$DN_i = \sum_{k=1}^n f_k DN_{ik} + \varepsilon_i \quad (1)$$

where 'DN_i' is the encoded radiance of each pixel in band i.

'DN_{ik}' is the pure reflectance of image endmember k in band i.

'f_k' is the fraction of each endmember k in any pixel. It will be the same for each band.

'i' is the band number.

'k' is the endmember number from '1' to 'n'.

'ε_i' is the remainder between measured and modeled DN (residual).

Fractions of endmembers are summed to be 1 for each pixel.

$$\sum_{k=1}^n f_k = 1 \quad (2)$$

Root Mean Square Error (RMSE) used to assess the fit of the model for all pixels in the image can be computed by the following equation.

$$RMSE = \sqrt{\frac{\sum_{i=1}^n (\varepsilon_i)^2}{n}} \quad (3)$$

ε_i is the difference between DN from the image and DN from the model of each pixel in the image. 'n' is the number of bands used in the model. The less RMSE indicates the better fit of the model.

Data Processing

Geometric Correction

The Landsat5 TM images covering the study area, supported by Geo-Informatics and Space Technology Development Agency (Public Organization) or GISTDA, were acquired on 6 March 2005 (Systematic Geo-correction

product of path 128 rows 50) in the dry season with clear sky conditions. The image data were rectified by use of color air photos with a scale of 1:25,000 and coordinate system of UTM WGS 1984 zone 48 north. The root mean square error (RMSE) obtained from the rectification process is 0.665 pixel or 16.63 m. A nearest neighborhood algorithm was used to resample the images to 25m × 25m pixel size.

Endmember Selection

The PCA was applied to transform 6 reflection bands of Landsat 5 TM data (excluding the thermal band) to 6 principal component images. The eigen values of component 1 to 6 are 1131.57, 108.17, 90.98, 14.21, 9.46, and 1.06, respectively. The percent of total variance explained by the components are 83.48, 7.98, 6.71, 1.05, 0.84, and 0.08. It means that, for example, the first principle component accounts for 83.48% of the variance in that 6-band data set and component 2 accounts for 7.98% of the remaining variance. The first 3 components with higher percent of total variance were used for endmember selection. The unique spectral signatures of 4 endmembers which were soil, shade, green vegetation, and impervious surface were picked from the scatter-plots of the first 3 principle component images as shown in Figure 4. The unique signatures show narrow standard deviations. The spectral signature of shade mostly matches to water bodies within the study area. The unique or pure signature pixels of the soil, shade, green vegetation, and impervious surface endmembers were in turn used as the AOI (area of interest) in the LSMA model.

Fraction Image Generation

The unique signatures of those 4 endmembers of each TM band were separated into 2 different sets of combinations: a) the 3 endmember combination of green vegetation, impervious surface, and soil (V-I-S), and b) the 3 endmember combination of green vegetation, soil, and shade (V-S-Sh). Each set was input to the LSMA function of ENVI version 4.2 to attain a fraction image of each endmember. Each pixel of a certain image contains a value indicating the proportionate area covered by a

certain endmember. Results of LSMA were fraction images of V-I-S and V-S-Sh sets (Figure 5) and its RMSE images. The mean RMSE was 2.16 and 2.38 for V-I-S and V-S-Sh respectively. The bright area shows a high percentage of a certain fraction and the darker gray shows a lower percentage. For example, Figure 5(b) illustrating the impervious fraction image of the V-I-S combination, road and structure areas appears bright which means that those pixels contain a high percentage of impervious surfaces and a low percentage of green vegetation and soil.

Fraction Images Classification

MLC and EMC were 2 methods used for urban classifications in the research. MLC is the well-know conventional method. EMC defines the composition limits of 3 endmembers (from fraction images) of each land-use class by performing a pixel-based ternary plot of those compositions obtained from training areas of certain classes. The ternary plot was performed in a triangular shape used to present the relative percentage of 3 components summed up to 100%. The plotted point data in a ternary diagram tend to separate to be clusters

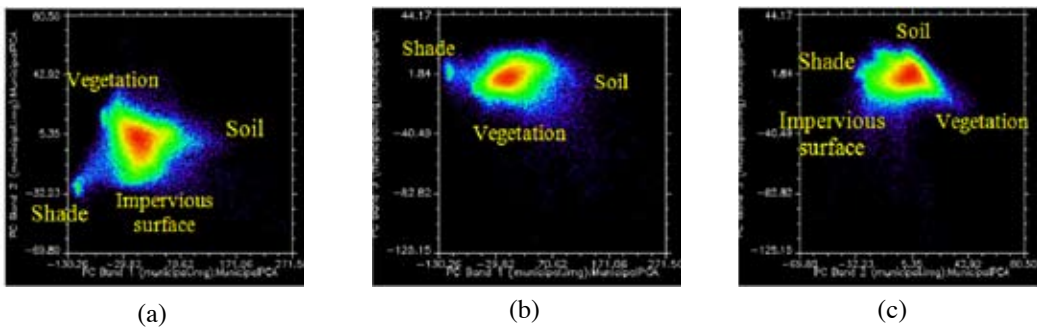


Figure 4. Scatter-plots of principal component images between: (a) PC1 and PC2, (b) PC1 and PC3, and (c) PC2 and PC3

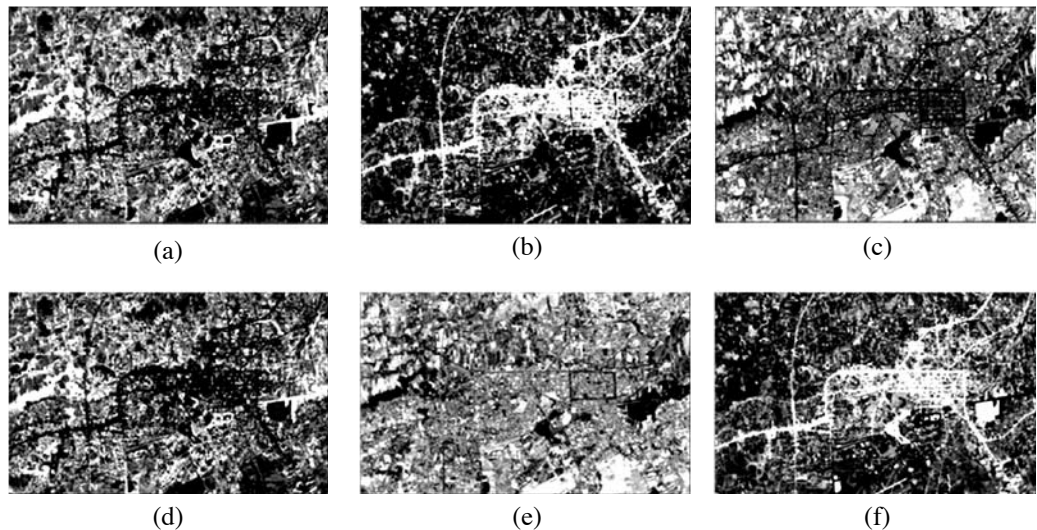


Figure 5. Example of the (a) green vegetation, (b) impervious surface, and (c) bare soil using V-I-S, and (d) green vegetation, (e) soil, and (f) shade using V-S-Sh of the study area

of certain classes. Therefore, a certain class will have its own frame/limit, as in the examples shown in Figure 6. Then, each pixel of a set of fraction images was plotted in the ternary model and classified to be a land-use class based on composition limits in the model. To this end, every classified unit was further combined to be a land-use map.

The MLC was used to classify the original Landsat TM images, fraction images of V-I-S, and V-S-Sh. The EMC was used to classify only fraction images of V-I-S and V-S-Sh. This resulted in a total 5 land-use maps (Figure 7). The original Landsat TM images were classified into 8 classes according to the training areas selected. Fraction images of V-I-S and V-S-Sh were classified into 7 classes excluding water.

Results of the land-use classifications are shown in Table 1. Percentages of the covering area of each class from each map of different classification methods were summarized. Residential areas, shrub, CBD, and grass field/bare soil (G/B) almost equally share the main part of the study area followed by a considerable part of horticultural area and less paddy field and forest. This implies that this study area is not an ordinary urban area because in general an urban area will obviously consist more of CBD and residential areas than other types. Therefore, the discussion on the accuracy of the maps is more focused on CBD and residential areas which should be a major part of any urban area. G/B and shrub could be considerable parts in any developing

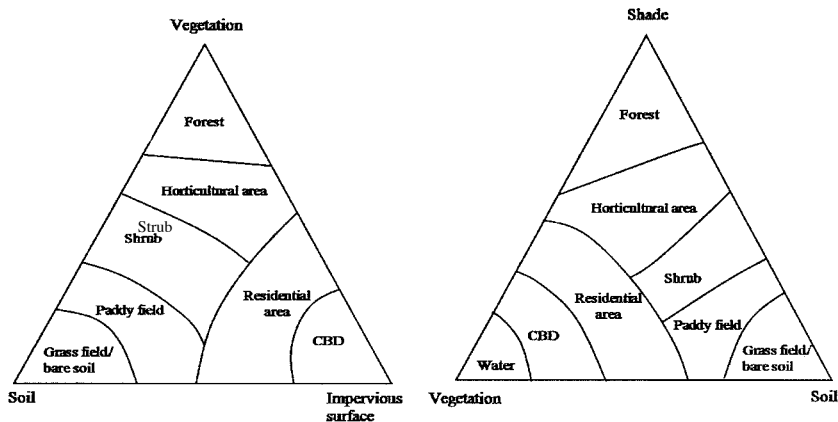


Figure 6. Ternary diagram of V-I-S and V-S-Sh combination sets for EMC

Table 1. Summarized percentages of covering area of each class from each map of different classification methods

Classification method of images	CBD	Residential area	G/B	Shrub	Horticultural area	Forest	Paddy field	Water
MLC of TM	16.1	21.3	12.2	18.2	7.6	3.8	18.5	2.2
MLC of V-I-S	12.0	22.4	13.9	18.3	12.7	11.4	9.3	-
MLC of V-S-Sh	11.9	15.0	25.8	17.1	25.8	9.3	7.3	2.4
EMC of V-I-S	8.8	14.4	6.1	18.4	30.8	14.2	7.4	-
EMC of V-S-Sh	7.9	20.4	11.5	13.5	14.5	13.3	17.4	1.4

urban area as well.

Accuracy Assessment of Land-use Maps

Accuracies of the 5 land-use maps, which are products of pairs of different data and classification methods, were assessed using an error matrix to determine the overall accuracy and Kappa statistic (Table 2), and the producer’s and user’s accuracies (PA and UA) of each class (Table 3) with the reference data from color air photos and field survey. The number of samples used for the error matrix was assigned based on a multinomial distribution

function which is suitable for a thematic map with multiple classes (Jensen, 2005). It is noted that the total area of V-I-S fraction images is less than the original Landsat TM images because of its exclusion of water areas.

From Table 2, all land-use maps derived from fraction images show a higher overall accuracy and Kappa statistic than the one from the original TM images. This can confirm that fraction images obtained from the LSMA model carry higher potential than the TM

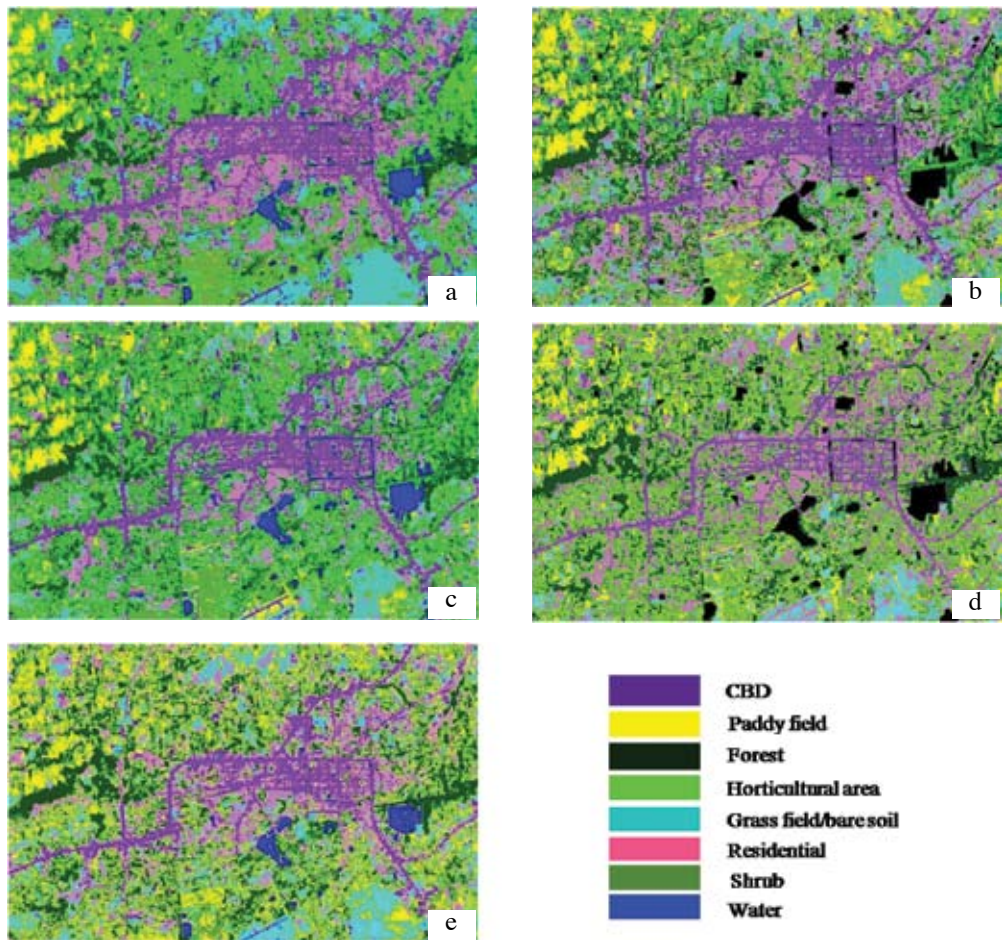


Figure 7. Land-use maps classified from original TM images, V-I-S and V-S-Sh fraction images by means of MLC and EMC methods

- (a) MLC of original TM images
- (b) MLC of V-I-S fraction images
- (c) MLC of V-S-Sh fraction images
- (d) EMC of V-I-S fraction images
- (e) EMC of V-S-Sh fraction images

images in applying to urban land-use classification. MLC of V-I-S shows the highest overall accuracy reaching to 72.21%. MLC of TM images show the lowest. However, different combinations of methods and fraction images show no obvious difference in the overall accuracy and Kappa statistic. Conclusively, V-I-S shows a hardly higher accuracy than V-S-Sh. MLC also shows a hardly higher

accuracy than EMC.

The accuracy, based on PA and UA, of classes of land-use maps is dependent on the image type and classification method. From Table 3, the accuracy comparison of some classes is discussed according to the different classification methods and sets of images used. These classes are CBD, residential area, G/B, and shrub which are more related to urban

Table 2. Summarized percentage of overall accuracy and Kappa statistic of each map classified using different sets of images and methods

Classification method and set of images	Overall accuracy	Kappa statistic
MLC of original TM images	66.93	62.20
MLC of V-I-S	72.21	67.50
MLC of V-S-Sh	67.05	62.30
EMC of V-I-S	68.44	63.20
EMC of V-S-Sh	69.15	64.70

Table 3. Summarized percentage of PA and UA of each land-use class for all classification methods

Classification method of images	CBD	Residential area	G/B	Shrub	Horticultural area	Forest	Paddy field	Water
rMLC of TM								
- PA	92.59	73.02	49.38	56.00	34.55	90.00	89.47	94.00
- UA	52.08	95.83	83.33	58.33	39.58	37.50	70.83	97.92
MLC of V-I-S								
- PA	100.00	87.04	54.22	58.57	55.00	100.00	85.71	-
- UA	83.64	85.45	81.82	74.55	60.00	54.55	65.45	-
MLC of V-S-Sh								
- PA	88.64	68.25	47.92	49.41	47.06	96.77	78.79	98.15
- UA	70.91	78.18	83.64	76.36	29.09	54.55	47.27	96.36
EMC of V-I-S								
- PA	96.67	70.89	60.75	49.41	55.36	91.43	78.72	-
- UA	86.57	83.58	97.01	62.69	46.27	47.76	55.22	-
EMC of V-S-Sh								
- PA	95.35	76.00	54.17	49.33	41.94	93.55	72.73	90.38
- UA	87.23	80.85	82.98	78.72	27.66	61.70	34.04	100.00

areas.

CBD - MLC of V-I-S, EMC of V-I-S, and EMC of V-S-Sh provide almost the same accuracy for this class. MLC of V-I-S provides 100% of PA and 83.64% of UA. It means that, using MLC, V-I-S fraction images can keep characteristics of this unit so well that all areas of the class were classified but they still carry other classes' characteristics similar to this class upto 16.36%, while EMC of V-S-Sh provides the highest UA (87.23%). It means that V-S-Sh is the best among the types of image in terms of least carrying other classes' characteristics that are similar to this class (12.77%).

Residential area - MLC of V-I-S, MLC of original TM, EMC of V-S-Sh, and EMC of V-I-S provide more to less accuracy to this class respectively. MLC of V-I-S provides the best PA (87.04%) and 85.45% UA. It means that, using MLC, V-I-S fraction images are the best to keep characteristics of this class so well that only 12.96% of this unit was misclassified but they still carry other classes' characteristic similar to this class upto 14.55%, while MLC of the original TM images provides the best UA (95.83%). It means that, using MLC, TM images are the best among the types of image in terms of least carrying other classes' characteristics that are similar to this class (only 4.17%).

G/B - EMC of V-I-S provides outstanding higher accuracy to this class than others which are about the same. This combination also provides the best PA (60.75%) and UA (97.01%). It means that, using EMC, V-I-S fraction images are the best to keep characteristics of this class so well that 39.25% of this class was misclassified and they carry only 2.99% of other classes' characteristics similar to this class.

Shrub - MLC of V-I-S provides higher a accuracy than others, followed by EMC of V-S-Sh and MLC of V-S-Sh. MLC of V-I-S provides the best PA (58.57%) and 74.55% UA. It means that, using MLC, V-I-S fraction images are the best to keep characteristics of this class so well that 41.43% of this class was misclassified but they still carry other classes'

characteristic similar to this class upto 25.45%, while EMC of V-S-Sh provides the best UA (78.72%). It means that, using EMC, V-S-Sh is the best among the types of image in terms of least carrying other classes' characteristics similar to this class (21.28%).

From the above discussion, the classes which are more related to urban areas are considered class by class. It reveals that the set of V-I-S fraction images shows a higher accuracy when applied to urban classification than the set of V-S-Sh and the original TM images, whereas no obvious difference of accuracies are shown between the usage of MLC and EMC.

Conclusions and Recommendation

Considering the overall accuracy and Kappa statistic, fraction images obtained from the LSMA model show a higher potential than the original TM images in being applied to urban land-use classification of the study area. When CBD, residential area, G/B, and shrub are considered class by class, the set of V-I-S fraction images shows a higher accuracy than the set of V-S-Sh and original TM images. There is no obvious difference in accuracies when the MLC and EMC methods are employed.

It is noted that the accuracy achieved from the study is still lower than those of other researches using the same method such as the one of Lu and Weng (2004) in which the overall accuracy can reach to 89.33%. The characteristics of the study areas could cause the significant difference of results of this research and others. Most researchers used a metropolitan city as a study area such as Indianapolis (Lu and Weng, 2004, 2006) and the metropolitan area of Columbus, Ohio (Wu and Murray, 2003; and Wu, 2004). Those areas have well developed systematic and zonal management. Their CBDs are always located as the centers which are clearly separated from other classes. Residential areas are also developed clearly as zones. In contrast, in this study area, residential areas are always mixed with CBD, industrial, and

even horticultural areas. This can result in decreasing the classification accuracy.

For further study, endmember selection needs to be improved because RMSEs are too high (2.16 for V-I-S and 2.38 for V-S-Sh) compared with other researches. According to Wu (2004), the brightness normalization method was applied to reduce the brightness variation of images. This could help increase the ability in selecting pure endmember signatures more precisely. Additionally, to increase the accuracy of land-use classification, census data could be used to be incorporated with the LSMA method (Lu and Weng, 2006). These 2 additional techniques are here recommended for further study.

Acknowledgement

The authors greatly appreciate GISTDA in supporting the Landsat TM images covering the study area to allow this research to be possible. The authors also wish to thank the Suranaree University of Technology for providing a part of the research funding.

Reference

- Adams, J.B., Sabol, D.E., Kapos, V., Filho, R.A., Roberts D.A., Smith, M.O., and Gillespie, A.R. (1995). Classification of multispectral image based on fraction endmembers: application to land cover change in the Brazilian Amazon. *Remote Sens. Environ.*, 52:137-154.
- Jensen, J.R. (2005). *Introductory Digital Image Processing: A Remote Sensing Perspective*. 3rd ed. Prentice Hall, Upper Saddle River, NJ, USA, 318p.
- Kulrat, C. (2008). Sub-pixel classification of urban area using fraction images from multi-endmember spectral analysis: Amphoe Muang Nakhon Ratchasima, [M.Sc. thesis]. School of Remote Sensing, Institute of Science, Suranaree University of Technology. Nakhon Ratchasima, Thailand, 81p.
- Lu, D. and Weng, Q. (2004). Spectral mixture analysis of the urban landscape in Indianapolis City with Landsat ETM⁺ Imagery. *Photogramm. Eng. Rem. S.*, 70(9):1053-1062.
- Lu, D. and Weng, Q. (2006). Use of impervious surface in urban land-use classification. *Remote Sens. Environ.*, 102:146-160.
- Lu, D., Moran, E., and Batistella, M. (2003). Linear mixture model applied to amazon vegetation classification. *Remote Sens. Environ.*, 87:456-469.
- Phinn, S., Stanford, M., Scarth, P., Murray, A.T., and Shyy, T. (2002). Monitoring the composition and form of urban environments based on the vegetation-impervious surface-soil (V-I-S) model by sub-pixel analysis techniques. *Int. J. Remote Sens.*, 23(20):4131-4153.
- Plaza, A., Martínez, P., Pérez, R., and Plaza, J. (2002). Spatial/Spectral endmember extraction by multidimensional morphological operations. *IEEE T. Geosci. Remote*, 40(9):2025-2041.
- Ridd, M.K. (1995). Exploring a V-I-S (Vegetation-Impervious surface-Soil) Model for urban ecosystem analysis through remote sensing: comparative anatomy for cities. *Int. J. Remote Sens.*, 16:2165-2185.
- Small, C. (2001). Estimation of Urban Vegetation Abundance by Spectral Mixture Analysis. *Int. J. Remote Sens.*, 22:1305-1334.
- Wu, C. (2004). Normalized spectral mixture analysis for monitoring urban composition using ETM⁺ imagery. *Remote Sens. Environ.*, 93:480-492.
- Wu, C. and Murray, A.T. (2003). Estimating impervious surface distribution by spectral mixture analysis. *Remote Sens. Environ.*, 84:493-505.

